NASA TECHNICAL NOTE

NASA TN D-3504

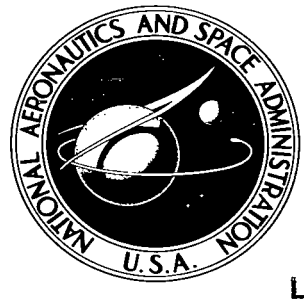

NASA TN D-3504

RADIATION FROM A SLOT ANTENNA IN A GROUND PLANE COVERED BY A WARM PLASMA LAYER

by Norman C. Wenger

Lewis Research Center

Cleveland, Ohio

NATIONAL AERONAUTICS AND SPACE ADMINISTRATION • WASHINGTON, D. C. • JULY 1966

NASA TN D-3504

RADIATION FROM A SLOT ANTENNA IN A GROUND PLANE COVERED BY A WARM PLASMA LAYER

By Norman C. Wenger

Lewis Research Center
Cleveland, Ohio

NATIONAL AERONAUTICS AND SPACE ADMINISTRATION

For sale by the Clearinghouse for Federal Scientific and Technical Information
Springfield, Virginia 22151 – Price $2.00

CONTENTS

RADIATION FROM A SLOT ANTENNA IN A GROUND PLANE COVERED BY A WARM PLASMA LAYER*

by Norman C. Wenger

Lewis Research Center

SUMMARY

The electromagnetic properties of a model of a reentry plasma layer are determined by using the linearized hydrodynamic equations for a single fluid warm plasma medium. The model consists of a perfectly conducting plane of infinite extent covered by a warm plasma layer of uniform density. The field excited by a slot antenna in the conducting plane is computed by using Fourier transform techniques. Expressions are obtained for the radiation field and for the waves guided along the plasma layer. Numerical results are presented that show the dependence of the energy transport by the field on frequency and electron temperature. In addition, the radiation pattern of the far-zone field is computed for various frequencies and electron temperatures.

INTRODUCTION

A considerable amount of research has been done in recent years on the electromagnetic aspects of space flight. The particular subject that has perhaps received the greatest attention is the effect on communication systems of the ionized gas layer that envelops a reentry vehicle. In a typical reentry situation, the ionized gas layer attenuates radio signals to such an extent as to cause a communications blackout. It is, therefore, of prime importance to understand reentry phenomena as completely as possible in order to develop methods to alleviate the blackout problem.

The proposed solutions of the blackout problem can generally be grouped into two categories. In the first group are those methods that attempt to alter the ionized

---

*Portions of this report were included in a thesis submitted to Case Institute of Technology, Cleveland, Ohio, May 1965 in partial fulfillment of the requirements for the degree of Doctor of Philosophy.

gas layer by injecting a chemical into it in order to produce electron attachment or to hasten the recombination processes (ref. 1). The second group contains those methods whereby a magnetic field is impressed upon the ionized layer in order to make it more transparent to electromagnetic radiation (ref 2). Before the effectiveness of any of these methods can be determined, it is necessary to have a valid model of the ionized layer.

The majority of the theoretical analyses on the effect of an ionized gas on electromagnetic radiation use the cold plasma model. A common configuration employed in the treatment of the reentry problem consists of a perfectly conducting plane covered by a cold plasma layer of uniform density. The source for the electromagnetic radiation is usually a slot antenna in the conducting plane. An extensive account of the major phenomena observed for this model appears in references 3 to 5. The results of these investigations indicate that the cold plasma layer has a very small effect on the electromagnetic radiation for frequencies sufficiently above the plasma frequency. At frequencies near or below the plasma frequency, severe distortion or attenuation of the radiation field is present. In addition, there may be waves trapped by the plasma layer. Some of these trapped waves exhibit very unusual properties such as being backward waves. A knowledge of the properties of these waves is extremely important in determining the efficiency of an antenna system since these trapped waves may transport a considerable amount of energy.

One of the main criticisms that can be made against the use of the cold plasma model in connection with reentry studies is that the very mechanism that produces the plasma, namely, high temperature, has been neglected. Some work has been done that uses the warm plasma model. Stewart and Caron (ref. 6) have computed the radiation from a line source in a ground plane covered by a warm plasma layer. The results of their analysis are, however, limited by an approximation that requires the source frequency to be near the plasma frequency.

This investigation presents an exact analysis of a model of a warm reentry plasma layer to determine the effect of the plasma temperature. The total field excited by a slot antenna in a conducting plane covered by a warm plasma layer is computed by using Fourier transform techniques. Expressions are obtained for the far-zone radiation field and for the waves guided by the plasma layer. The energy transported by the radiation field and by each of the guided waves is computed. The spectrum of waves associated with a plasma layer is shown to be significantly changed by the nonzero plasma temperature. The effect of the temperature is to generate a completely new spectrum of guided waves that are electroacoustic in nature in addition to perturbing the waves associated with the cold plasma layer.

This research was partly supported by the Air Force Cambridge Research Laboratories, Office of Aerospace Research, under contract AF 19(628)-1699.

SYMBOLS

a	acoustic velocity in electron gas
$\hat{a}_x, \hat{a}_y, \hat{a}_z$	unit vectors in x-, y-, and z-directions
b	plasma layer thickness
C	inversion contour (fig. 2)
c	velocity of light
$D(\beta)$	see equation (35g)
d	width of slot antenna
$\overline{E}$	total electric field intensity
$\overline{e}$	perturbation electric field intensity
$\overline{F}$	long-range force acting on electrons
$\overline{H}$	total magnetic field intensity
$\mathcal{H}$	Fourier transform of h_y
$\overline{h}$	perturbation magnetic field intensity
h_y	y-component of $\overline{h}$
Im	imaginary part of
I_m	magnetic current
$\overline{J}$	total electric current density
$\overline{J}_m$	total magnetic current density
$\overline{j}_m$	perturbation magnetic current density
k	Boltzmann constant
k_e	wave number for magnetic field in plasma
k_o	free-space wave number
k_p	wave number for pressure field in plasma
$M(x, \beta)$	see equation (35f)
m	mass of electron

N	total electron number density
$N(x, \beta)$	see equation (35e)
n	perturbation electron number density
n_o	equilibrium electron number density
P	total electron pressure
$\mathscr{P}$	Fourier transform of p
p	perturbation electron pressure
p_o	equilibrium electron pressure
q	electronic charge
Re	real part of
r	radial coordinate (fig. 1)
$\overline{r}$	general position vector
$\overline{S}$	energy flux vector
T_e	electron temperature
t	time
$u(z)$	unit step function
$\overline{V}$	total electron fluid velocity
$\overline{v}$	perturbation electron fluid velocity
x, y, z	rectangular coordinates (fig. 1)
α	$(\beta^2 - k_o^2)^{1/2}$
β	Fourier transform variable
β_n	n^{th} root of $D(\beta) = 0$
Γ_h	transverse wave number for magnetic field in plasma
Γ_p	transverse wave number for pressure field in plasma
γ	ratio of specific heats with constant pressure to constant volume of electron gas
$\delta(x)$	delta function
ϵ_o	electric permittivity of free space

ϵ_p relative dielectric constant of plasma

η imaginary part of ν

θ polar coordinate

θ_c critical angle associated with magnetic field

θ_o critical angle associated with pressure field

λ_g wavelength of guided waves in plasma

λ_o free-space wavelength

λ_p free-space wavelength at plasma frequency

μ_o magnetic permeability of free space

ν complex variable

ρ modulus of $\nu - (\pi/2 - \theta)$

σ real part of ν

φ phase of $\nu - (\pi/2 - \theta)$

ω source frequency

ω_p plasma frequency

$*$ complex conjugate

BASIC EQUATIONS FOR A WARM PLASMA

A plasma can be considered as being comprised of several miscible fluids. These fluids will consist, in general, of an electron fluid, an ion fluid for each species of ion, and a neutral particle fluid for each species of neutral particle. The dynamics of these fluids will be described by the basic hydrodynamic equations. An excellent discussion on the validity of the hydrodynamic treatment has been given by Oster (ref. 7).

In order to simplify the analysis of a warm plasma, it will be assumed that the time variation of all nonstationary quantities is sufficiently rapid so that only the electron motion need be considered. This assumption allows the plasma to be described by the single electron fluid model. For this case, the transport equations of interest are

$$\frac{\partial N}{\partial t} + \nabla \cdot (N\overline{V}) = 0 \tag{1}$$

$$mN \frac{\partial \overline{V}}{\partial t} + mN(\overline{V} \cdot \nabla)\overline{V} = N\overline{F} - \nabla P \tag{2}$$

$$PN^{-\gamma} = \text{constant} \tag{3}$$

where

$N(\overline{r}, t)$ electron number density

$\overline{V}(\overline{r}, t)$ electron fluid velocity

$P(\overline{r}, t)$ electron pressure

$\overline{F}(\overline{r}, t)$ long-range force per electron

γ ratio of specific heat with constant pressure to specific heat with constant volume of electron gas

m mass of electron

Equations (1) to (3) are a statement of the conservation of matter, conservation of momentum, and conservation of energy of the electrons, respectively. Dissipative effects such as collisions between the electrons and ions have been neglected to simplify the analyis.

Maxwell's equations must be employed to complete the description of the dynamics of a warm plasma:

$$\nabla \times \overline{H} = \overline{J} + \epsilon_o \frac{\partial \overline{E}}{\partial t} \tag{4}$$

$$\nabla \times \overline{E} = -\overline{J}_m - \mu_o \frac{\partial \overline{H}}{\partial t} \tag{5}$$

The new symbols used are

$\overline{J}(\overline{r}, t)$ electric current density

$\overline{J}_m(\overline{r}, t)$ magnetic current density

$\overline{H}(\overline{r}, t)$ magnetic field intensity

$\overline{E}(\overline{r}, t)$ electric field intensity

ϵ_o electric permittivity of free space

μ_o magnetic permeability of free space

The electromagnetic equations have been formulated so that the electric current density $\overline{J}$ includes all conduction, convection, and polarization currents in the plasma. A magnetic current density $\overline{J}_m$ has been included in equation (5) since it provides an easy way to introduce the effect of the slot antenna later.

The hydrodynamic equations and the electromagnetic equations are coupled by the force $\overline{F}$ and the current density $\overline{J}$. If gravitational fields are neglected, $\overline{F}$ can be given by the Lorentz force equation

$$\overline{F} = q(\overline{E} + \overline{V} \times \mu_o \overline{H}) \tag{6}$$

where q is the charge on the electron. The current density $\overline{J}$ is given by

$$\overline{J} = qN\overline{V} \tag{7}$$

for the case where the conduction and polarization currents do not exist. This situation will prevail if there are no electric current sources within the plasma and if the polarization field of the neutral particles and ions is negligible compared with the applied field.

Equations (1) to (7) represent 17 scalar equations in the eight variables $\overline{E}$, $\overline{H}$, $\overline{V}$, $\overline{F}$, $\overline{J}$, $\overline{J}_m$, P, and N, which constitute 20 scalars. If the magnetic current density $\overline{J}_m$ is specified, equations (1) to (7) form a complete set of equations for the description of the dynamics of a warm plasma.

At this point, the equations will be linearized by expressing the variables as the sum of a static term plus a small time-varying perturbation term. Thus,

$$\overline{E}(\overline{r}, t) = \overline{e}(\overline{r})e^{i\omega t} \tag{8a}$$

$$\overline{H}(\overline{r}, t) = \overline{h}(\overline{r})e^{i\omega t} \tag{8b}$$

$$\overline{V}(\overline{r}, t) = \overline{v}(\overline{r})e^{i\omega t} \tag{8c}$$

$$\overline{J}_m(\overline{r}, t) = \overline{j}_m(\overline{r})e^{i\omega t} \tag{8d}$$

$$N(\bar{r}, t) = n_o(\bar{r}) + n(\bar{r})e^{i\omega t} \tag{8e}$$

$$P(\bar{r}, t) = p_o(\bar{r}) + p(\bar{r})e^{i\omega t} \tag{8f}$$

where a time variation of $e^{i\omega t}$ has been used for all nonstationary quantities. The total $\bar{E}$, $\bar{H}$, $\bar{V}$, and $\bar{J}_m$ fields are assumed to consist of only perturbation quantities. The quantities $n_o(\bar{r})$ and $p_o(\bar{r})$ represent the equilibrium electron density and pressure, respectively.

Substituting equations (8a) to (8f) into (1) to (7) yields the following set of equations:

$$i\omega n + \nabla \cdot (n_o \bar{v}) = 0 \tag{9a}$$

$$i\omega m n_o \bar{v} = n_o q \bar{e} - \nabla p \tag{9b}$$

$$p = \frac{\gamma p_o}{n_o} n \tag{9c}$$

$$\nabla \times \bar{h} = n_o q \bar{v} + i\omega \epsilon_o \bar{e} \tag{9d}$$

$$\nabla \times \bar{e} = -\bar{j}_m - i\omega \mu_o \bar{h} \tag{9e}$$

The factor $e^{i\omega t}$ has been suppressed in the preceding equations. In obtaining equations (9a) to (9e), all products of perturbation terms have been neglected in order to make the equations linear.

Equations (2) and (8f) force the equilibrium electron pressure $p_o(\bar{r})$ to be a constant. Consequently, the equilibrium electron density $n_o(\bar{r})$ must also be a constant since the pressure and density are related by an equation of state. The requirement that the equilibrium density be uniform is a direct result of neglecting ionization and recombination. The random motion of the electrons due to the nonzero electron temperature will distribute the electrons uniformly in space unless there is a source or sink of electrons.

The quantity $a^2 = \gamma p_o / n_o m$ in equation (9c) can be identified as the square of the adiabatic acoustic velocity for the electron gas. If the electron gas obeys the equation of state for an ideal gas, a^2 is given by

$$a^2 = \frac{\gamma k T_e}{m}$$

where k is the Boltzmann constant, and T_e is the electron temperature.

Since the perturbation electron pressure and density are proportional, equations (9a) to (9e) can be reduced to the following set:

$$i\omega p + mn_o a^2 \nabla \cdot \bar{v} = 0 \tag{10a}$$

$$i\omega m n_o \bar{v} = n_o q \bar{e} - \nabla p \tag{10b}$$

$$\nabla \times \bar{h} = n_o q \bar{v} + i\omega \epsilon_o \bar{e} \tag{10c}$$

$$\nabla \times \bar{e} = -\bar{j}_m - i\omega \mu_o \bar{h} \tag{10d}$$

Equations (10a) to (10d) are the basic equations for a warm plasma. The standard equations that describe a cold plasma can be obtained from the preceding set by setting the pressure equal to zero.

The basic equations can be put into a more tractable form by combining equations (10a) to (10d) to give

$$\nabla \times \nabla \times \bar{h} - k_e^2 \bar{h} = -i\omega \epsilon_o \epsilon_p \bar{j}_m \tag{11}$$

$$\nabla^2 p + k_p^2 p = 0 \tag{12}$$

$$\bar{e} = -\frac{i}{\omega \epsilon_o \epsilon_p} \nabla \times \bar{h} - \frac{q}{\omega^2 \epsilon_o \epsilon_p m} \nabla p \tag{13}$$

$$\bar{v} = -\frac{q}{\omega^2 \epsilon_o \epsilon_p m} \nabla \times \bar{h} + \frac{i}{\omega \epsilon_p n_o m} \nabla p \tag{14}$$

The new symbols introduced are $\omega_p^2 = n_o q^2 / \epsilon_o m$, the square of the electron plasma frequency, $\epsilon_p = 1 - \omega_p^2 / \omega^2$, the effective relative dielectric constant of the plasma, $k_e^2 = \epsilon_p \omega^2 / c^2$, and $k_p^2 = \epsilon_p \omega^2 / a^2$.

The previous equations show that the solution for the field in a warm plasma medium can be obtained if $\bar{j}_m$ is known by first solving equations (11) and (12) for $\bar{h}$ and p and then using equations (13) and (14) to compute $\bar{e}$ and $\bar{v}$.

THE MODEL

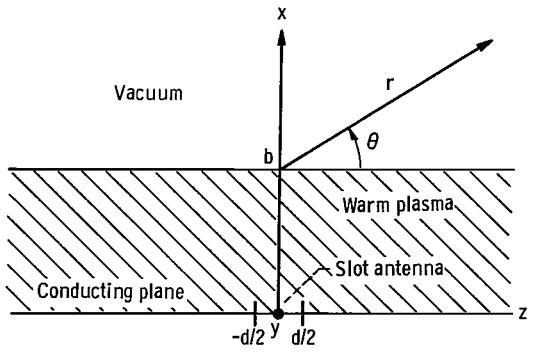

Figure 1. - Model of reentry plasma layer.

The plasma layer surrounding a reentry vehicle has a very complex structure. The electron density and pressure possess both spatial and time variations. In order to obtain a model that can be analyzed exactly, several simplifying assumptions must be made.

Figure 1 shows the model that will be considered. The surface of the space vehicle will be approximated by a plane of infinite extent and of infinite electrical conductivity. The case where the plane is finite in length has been treated by Oliner and Tamir (ref. 8) using the cold plasma model. Their results indicate that, as long as the source of the electromagnetic radiation is at least 10 wavelengths from the nearest edge of the plane, the infinite plane will represent a valid approximation of a finite plane. In practice, the surface of a space vehicle is usually cylindrical. However, if the radius of curvature of the surface is much larger than 1 wavelength, the infinite plane model should give useful results.

The source for the electromagnetic radiation will be a uniformly excited slot antenna of width d and of infinite extent located on the conducting plane. The infinite extent of the antenna simplifies the problem by making it two dimensional.

The plasma layer surrounding the reentry vehicle will be approximated by a plasma slab of uniform density in the region $0 < x < b$. The remaining region $x > b$ is assumed to be a vacuum. A plasma slab of this form could never exist in practice unless some confining mechanism were provided at the discontinuity in the electron density along the surface $x = b$. However, the slab configuration does provide a useful mathematical model.

In the previous section, it was shown that, in a warm plasma medium, the equilibrium electron density must be constant if ionization and recombination are absent. The most general equilibrium density variation that can be used in conjunction with the previously developed equations is one that is uniform in space except for possible step discontinuities along a surface. Therefore, the most general plasma slab that could be considered would be multilayered. The thickness, density, and temperature of each layer could be specified to give the best approximation of the actual density-temperature profile. However, in the interest of simplicity, only the single-layered plasma slab will be considered in this analysis.

The electrical characteristics of the model can be completely specified by the dimensionless parameters $\omega_p b/c$, $\omega d/c$, a/c, and ω_p/ω. In practice, the numerical values of these parameters will have wide variations that depend on the configuration of the

space vehicle and its reentry trajectory. Typical ranges of values of these parameters for space vehicles such as Mercury, Gemini, and Apollo are $0 < \omega_p b/c < 20$, $0 < a/c < 2\times10^{-3}$, and $0 < \omega_p/\omega < 5$. The value $\omega_p b/c = 20$ corresponds to a plasma layer thickness of $3\lambda_p$, where λ_p is the free-space wavelength at the plasma frequency, and the value $a/c = 2\times10^{-3}$ corresponds to an electron temperature of 15×10^3 °K. A typical value for $\omega d/c$ is 0.5, which corresponds to a slot width of 0.1 λ_o, where λ_o is the free-space wavelength at the operating frequency.

BOUNDARY CONDITIONS

Before a formal solution for the field can proceed, it is necessary to select a set of boundary conditions for the field components. The boundary conditions that are selected should satisfy the physics of the problem as closely as possible and also require the solution for the field to be unique. A systematic method for making this selection is first to determine all the possible sets of boundary conditions that will yield a unique solution and then choose the set that conforms to the physical problem as closely as possible.

First, consider the plasma region $0 < x < b$. The magnetic field in this region satisfies the differential equation (eq. 11), which is repeated here for convenience:

$$\nabla \times \nabla \times \bar{h} - k_e^2 \bar{h} = -i\omega\epsilon_o\epsilon_p \bar{j}_m \tag{11}$$

It is assumed that $\bar{j}_m$ is known. Let $\bar{f}$ be an arbitrary vector function. Scalar multiplying equation (11) by $\bar{f}$ gives

$$\bar{f} \cdot \nabla \times \nabla \times \bar{h} - k_e^2 \bar{f} \cdot \bar{h} = -i\omega\epsilon_o\epsilon_p \bar{f} \cdot \bar{j}_m \tag{15}$$

By using the vector identity

$$\bar{f} \cdot \nabla \times \nabla \times \bar{h} = (\nabla \times \bar{h}) \cdot (\nabla \times \bar{f}) + \nabla \cdot [(\nabla \times \bar{h}) \times \bar{f}]$$

equation (15) can be rewritten in the following form:

$$(\nabla \times \bar{h}) \cdot (\nabla \times \bar{f}) - k_e^2 \bar{f} \cdot \bar{h} + \nabla \cdot [(\nabla \times \bar{h}) \times \bar{f}] = i\omega\epsilon_o\epsilon_p \bar{f} \cdot \bar{j}_m \tag{16}$$

Let both $\bar{h}_1$ and $\bar{h}_2$ be solutions of equation (11). Then $\bar{h}_d = \bar{h}_1 - \bar{h}_2$ is a solution of the associated homogeneous equation. Thus,

$$(\nabla \times \bar{h}_d) \cdot (\nabla \times \bar{f}) - k_e^2 \bar{f} \cdot \bar{h}_d + \nabla \cdot [(\nabla \times \bar{h}_d) \times \bar{f}] = 0 \tag{17}$$

Now let $\bar{f} = \bar{h}_d^*$ ($\bar{h}_d^*$ = complex conjugate of $\bar{h}_d$) and integrate equation (17) over the volume of the plasma V_p:

$$\int_{V_p} |\nabla \times \bar{h}_d|^2 \, dV - k_e^2 \int_{V_p} |\bar{h}_d|^2 \, dV + \oint_{S_p} (\nabla \times \bar{h}_d) \cdot (\bar{h}_d^* \times \hat{n}) dS = 0 \tag{18}$$

The divergence theorem has been used to reduce one of the volume integrals to a surface integral. The vector $\hat{n}$ is the unit normal to the surface S_p, which bounds V_p.

At frequencies below the plasma frequency, k_e^2 is negative. If the boundary conditions are selected so that the surface integral is positive definite, it must follow that $\bar{h}_d = 0$ or $\bar{h}_1 = \bar{h}_2$, since equation (18) consists of a sum of positive definite quantities equated to zero. Thus, the uniqueness of the magnetic field is ensured provided that the surface integral is positive definite. Two obvious choices for making this integral vanish would be to specify either $\hat{n} \times \bar{h}$ or $\hat{n} \times (\nabla \times \bar{h})$ on the surface of the plasma.

The boundary conditions for the uniqueness of the pressure field can be derived in an analogous manner. Let $p_d = p_1 - p_2$, where both p_1 and p_2 satisfy the differential equation for the pressure (eq. 12). By performing the obvious manipulations, it can be shown that

$$\int_{V_p} |\nabla p_d|^2 \, dV - k_p^2 \int_{V_p} |p_d|^2 \, dV - \oint_{S_p} p_d \frac{\partial p_d^*}{\partial n} \, dS = 0 \tag{19}$$

At frequencies below the plasma frequency, k_p^2 is negative. The boundary conditions that make the surface integral negative definite will require the pressure field to be unique. Two possible choices would be to specify either p or $\partial p/\partial n$ on the surface of the plasma.

The previous discussion shows that the field will be unique provided that the boundary conditions are selected so that the surface integrals that appear in equations (18) and (19) are positive and negative definite, respectively. The selection of a set of boundary conditions from the many possible sets revealed by uniqueness considerations is determined, of course, by the physics of the problem. The usual boundary conditions for the electromagnetic field should apply in this problem. Along the surface of the perfect conductor, the tangential component of the electric field must vanish It is readily apparent from equation (13) that the condition $\hat{n} \times \bar{e} = 0$ at $x = 0$ is equivalent to

$$\hat{n} \times (\nabla \times \bar{h})\Big|_{x=0} = \frac{iq}{\omega m} \hat{n} \times \nabla p\Big|_{x=0} \tag{20}$$

where $\hat{n} = \hat{a}_x$. At the plasma-vacuum interface, the tangential components of both the electric and the magnetic field vectors must be continuous. Again, from equation (13), the requirement that both $\hat{n} \times \bar{e}$ and $\hat{n} \times \bar{h}$ be continuous at $x = b$ is equivalent to

$$\hat{n} \times (\nabla \times \bar{h}) - \frac{iq}{\omega m} \hat{n} \times \nabla p\Big|_{x=b^-} = \epsilon_p \hat{n} \times (\nabla \times \bar{h})\Big|_{x=b^+} \tag{21}$$

and

$$\hat{n} \times \bar{h}\Big|_{x=b^-} = \hat{n} \times \bar{h}\Big|_{x=b^+} \tag{22}$$

where $\hat{n} = \hat{a}_x$. Thus, the boundary conditions (20) to (22) will specify $\hat{n} \times (\nabla \times \bar{h})$ on the surface of the plasma region provided that both the pressure field in the plasma and the electromagnetic field in the vacuum are known. It has already been shown that specifying $\hat{n} \times (\nabla \times \bar{h})$ on the surface of the plasma is a sufficient condition for the uniqueness of the magnetic field within the plasma.

The boundary conditions for the pressure are more difficult to select since the model under consideration is quite idealized. The possible choices of boundary conditions, however, can be grouped into two categories. In the first group are those boundary conditions that require the perturbation pressure to vanish on the surface of the plasma. This condition along with the boundary conditions for the electromagnetic field allow the magnetic and pressure fields to uncouple. Since the magnetic current does not appear as a source term in the pressure equation (eq. 12), the pressure field will not be excited. Therefore, this boundary condition for the pressure will simply yield the solution for the cold plasma model. All the other boundary conditions for the pressure will involve coupling between the magnetic and the pressure fields.

The boundary condition that will be used is

$$\hat{n} \cdot \bar{v}\Big|_{x=0,\, b^-} = 0 \tag{23}$$

with $\hat{n} = \hat{a}_x$. This boundary condition is obviously an approximation. It has, however, been widely used in the literature, which allows this analysis to be compared more easily with previous work.

Equation (23) can be put into the form

$$\left.\frac{\partial p}{\partial n}\right|_{x=0,\,b^-} = -\left.\frac{in_o q}{\omega\epsilon_o}\,\hat{n}\cdot\nabla\times\bar{h}\right|_{x=0,\,b^-} \tag{24}$$

by using equation (14). The boundary condition (24) specifies $\partial p/\partial n$ on the surface of the plasma provided that the magnetic field is known. It has been shown that specifying $\partial p/\partial n$ on the surface is a sufficient condition to ensure the uniqueness of the pressure field.

The previous discussion indicates that the boundary conditions that require the surface integrals in equations (18) and (19) to vanish are sufficient conditions for the uniqueness of the field within the plasma. The boundary conditions (20) to (22) and (24) make the surface integrals vanish over the surfaces $x = 0$ and $x = b$ of the plasma slab. However, to obtain physically meaningful solutions, the surface bounding the edge of the plasma slab at infinity must also be considered. The proper boundary condition to impose on this surface is a power radiation condition; that is, all waves at infinity should transport energy away from the source. A power-radiation condition must be imposed in lieu of the usual phase radiation condition since a plasma slab can support backward waves. A backward wave has its phase velocity and group velocity vectors in opposite directions so that a point on the wave of constant phase may be moving in the negative z-direction, for example, whereas the energy carried by the wave is transported in the positive z-direction. The power-radiation condition simply ensures that the net energy transport at infinity is directed away from the source.

So far, uniqueness conditions have been derived for the fields in the plasma region when the frequency is below the plasma frequency. At frequencies above the plasma frequency the proof is no longer valid. Resonant modes of arbitrary amplitude may exist when the relative dielectric constant of the plasma is positive. However, if an energy-loss mechanism such as collisions between the electrons and ions were introduced, the coefficients k_e^2 and k_p^2 in equations (18) and (19) would become complex with negative imaginary parts for all frequencies. This requires $p_d = 0$ and $\bar{h}_d = 0$, which ensures the uniqueness of the magnetic and pressure fields in the plasma.

The remaining point to consider is the uniqueness of the electromagnetic field in the vacuum region $x > b$. The magnetic field in this region satisfies the equation

$$\nabla\times\nabla\times\bar{h} - k_o^2\bar{h} = -i\omega\epsilon_o\bar{j}_m \tag{25}$$

where $k_o^2 = \omega^2/c^2$. (The equations that the field must satisfy in the vacuum region, i.e., Maxwell's equations, can, of course, be obtained from any of the previous sets of equations by systematically setting the equilibrium electron density equal to zero.) Following a procedure identical to that used to obtain equation (18) gives

$$\int_{V_v} \left|\nabla \times \bar{h}_d\right|^2 dV - k_o^2 \int_{V_v} \left|\bar{h}_d\right|^2 dV + \oint_{S_v} (\nabla \times \bar{h}_d) \cdot (\bar{h}_d^* \times \hat{n}) dS = 0 \qquad (26)$$

where V_v is the volume of the vacuum region $x > b$, and S_v is the boundary surface, which includes the plasma-vacuum interface and the surface at infinity. Since both $\hat{n} \times \bar{h}$ and $\hat{n} \times (\nabla \times \bar{h})$ are specified on the plasma-vacuum interface by equations (21) and (22), this portion of the surface integral will vanish. A sufficient condition to make the integral over the surface at infinity vanish is to impose the two-dimensional phase-radiation condition

$$\lim_{r \to \infty} r^{1/2} \left(\frac{\partial \bar{h}}{\partial r} + ik_o \bar{h} \right) = 0$$

where $r = \left[(x - b)^2 + z^2\right]^{1/2}$ for the model under consideration. This condition requires the field at great distances from the source to represent a divergent traveling wave. The phase-radiation condition is equivalent to a power-radiation condition in this case since backward waves no not exist in the vacuum region. If small losses were introduced into the medium, the imaginary part of k_o^2 in equation (26) would be negative at all frequencies. Thus, $\bar{h}_d = 0$, which ensures the uniqueness of the magnetic field in the vacuum.

The previous discussion indicates that the following boundary conditions are sufficient conditions for a unique solution and are those that will be used in the analysis:

(1) The component of the electric field tangent to the plasma surface must vanish at $x = 0$ and be continuous at $x = b$.

(2) The component of the magnetic field tangent to the plasma surface must be continuous at $x = b$.

(3) The component of the electron fluid velocity normal to the plasma surface must vanish at $x = 0$ and $x = b$.

(4) The total field must satisfy the proper phase or power-radiation condition at infinity.

FORMAL SOLUTION FOR THE FIELD

The formal solution for the field excited by the slot antenna will be determined by using Fourier transform techniques. It will be convenient to represent the slot antenna with a magnetic current. The field radiated by a uniformly excited slot antenna is identical to the field radiated by a uniform magnetic surface current on the aperture of the

antenna with the aperture closed by a perfectly conducting wall. The magnetic current density $\bar{j}_m$ can be expressed as

$$\bar{j}_m = \frac{I_m}{d}\left[u\left(z + \frac{d}{2}\right) - u\left(z - \frac{d}{2}\right)\right]\delta(x)\hat{a}_y \tag{27}$$

where I_m is the intensity of the total magnetic current.

An examination of the basic equation governing the magnetic field (eq. 11) reveals that the polarization of the magnetic field will be in the direction of the magnetic current $\bar{j}_m$, or in the y-direction for the coordinate system chosen. The other components of the magnetic field are not excited since the boundary conditions are invariant with respect to the y- and z-coordinates. Thus, the field components of interest will be the x- and z-components of the electric and velocity fields and the y-component of the magnetic field. The pressure will be a scalar function of the x- and z-coordinates. All other field components will vanish.

Let $\mathcal{H}(x,\beta)$ and $\mathcal{P}(x, \beta)$ be the Fourier transforms with respect to z of $h_y(x, z)$ and $p(x, z)$, respectively:

$$\mathcal{H}(x, \beta) = \int_{-\infty}^{\infty} h_y(x, z)e^{i\beta z}\, dz \tag{28a}$$

$$\mathcal{P}(x, \beta) = \int_{-\infty}^{\infty} p(x, z)e^{i\beta z}\, dz \tag{28b}$$

The functions $h_y(x, z)$ and $p(x, z)$ can then be recovered by the usual inversion integrals:

$$h_y(x, z) = \frac{1}{2\pi}\int_C \mathcal{H}(x, \beta)e^{-i\beta z}\, d\beta \tag{29a}$$

$$p(x, z) = \frac{1}{2\pi}\int_C \mathcal{P}(x, \beta)e^{-i\beta z}\, d\beta \tag{29b}$$

where C is a suitable contour in the complex β-plane. It is assumed that both the plasma and vacuum media have small losses so that the fields decay as $|z| \to \infty$. This is necessary to satisfy the uniqueness conditions and to allow the Fourier transforms to be taken. In obtaining numerical results, however, the losses will be neglected.

The Fourier transform with respect to z of the basic equations for the magnetic field and pressure (eqs. (11) to (14)) are easily seen to be

$$\frac{\partial^2 \mathcal{H}}{\partial x^2} + \left(k_e^2 - \beta^2\right)\mathcal{H} = i\omega\epsilon_o\epsilon_p I_m \frac{\sin\frac{\beta d}{2}}{\frac{\beta d}{2}}\delta(x) \qquad 0 < x < b \tag{30a}$$

$$\frac{\partial^2 \mathcal{P}}{\partial x^2} + \left(k_p^2 - \beta^2\right)\mathcal{P} = 0 \qquad 0 < x < b \tag{30b}$$

$$\frac{\partial^2 \mathcal{H}}{\partial x^2} + \left(k_o^2 - \beta^2\right)\mathcal{H} = 0 \qquad b < x \tag{30c}$$

$$\mathcal{P} = 0 \qquad b < x \tag{30d}$$

The right side of equation (30a) is recognized as being proportional to the Fourier transform of the magnetic current density given by equation (27). The boundary conditions given by equations (20) to (22) and (24) transform in a similar manner:

$$\frac{\partial \mathcal{H}}{\partial x} - \frac{q\beta}{\omega m}\mathcal{P}\Big|_{x=0} = 0 \tag{31a}$$

$$\frac{\partial \mathcal{H}}{\partial x} - \frac{q\beta}{\omega m}\mathcal{P}\Big|_{x=b^-} = \epsilon_p \frac{\partial \mathcal{H}}{\partial x}\Big|_{x=b^+} \tag{31b}$$

$$\mathcal{H}\Big|_{x=b^-} = \mathcal{H}\Big|_{x=b^+} \tag{31c}$$

$$\frac{\partial \mathcal{P}}{\partial x} - \frac{n_o q\beta}{\omega\epsilon_o}\mathcal{H}\Big|_{x=0} = 0 \tag{31d}$$

$$\frac{\partial \mathcal{P}}{\partial x} - \frac{n_o q\beta}{\omega\epsilon_o}\mathcal{H}\Big|_{x=b^-} = 0 \tag{31e}$$

In addition to the previous boundary conditions, the phase- or power-radiation conditions at infinity must also be imposed to specify the solution uniquely.

It will be convenient to include the effect of the magnetic surface current in the equations for the boundary conditions rather than in the differential equation for the magnetic field. This procedure is possible since the source for the field is located along one of the boundaries. Consider the surface current to be slightly elevated from the plane $x = 0$ so that $\delta(x)$ is replaced by $\delta(x - \epsilon)$ in equation (30a) where $\epsilon << b$. Since the magnetic field is continuous across the magnetic surface current, $\mathcal{H}(\epsilon^-, \beta)$ is equal to $\mathcal{H}(\epsilon^+, \beta)$. Therefore, the boundary condition (31d) is unchanged. The derivative of the magnetic field with respect to x is discontinuous, however, at $x = \epsilon$ by the amount $i\omega\epsilon_o\epsilon_p I_m\left(\sin\frac{\beta d}{2}\Big/\frac{\beta d}{2}\right)$. Thus, equation (31a) can be modified to read

$$\left.\frac{\partial \mathcal{H}}{\partial x} - \frac{q\beta}{\omega m}\mathcal{P}\right|_{x=0} = i\omega\epsilon_o\epsilon_p I_m \frac{\sin\frac{\beta d}{2}}{\frac{\beta d}{2}} \tag{32}$$

The solutions for the transformed variables $\mathcal{H}$ and $\mathcal{P}$ can now be determined where equation (30a) is regarded as homogeneous.

A general solution of equations (30a) to (30d) is given by

$$\mathcal{H} = H_o\left(e^{-i\Gamma_h x} + R_1 e^{i\Gamma_h x}\right) \qquad 0 < x < b \tag{33a}$$

$$\mathcal{P} = P_o\left(e^{-i\Gamma_p x} + R_2 e^{i\Gamma_p x}\right) \qquad 0 < x < b \tag{33b}$$

$$\mathcal{H} = H_o\left(e^{-i\Gamma_h b} + R_1 e^{i\Gamma_h b}\right)e^{-\alpha(x-b)} \qquad b < x \tag{33c}$$

$$\mathcal{P} = 0 \qquad b < x \tag{33d}$$

where

$$\Gamma_h \equiv \left(k_e^2 - \beta^2\right)^{1/2} \tag{34a}$$

$$\Gamma_p \equiv \left(k_p^2 - \beta^2\right)^{1/2} \tag{34b}$$

$$\alpha \equiv \left(\beta^2 - k_o^2\right)^{1/2} \tag{34c}$$

and H_o, P_o, R_1, and R_2 are complex functions of β to be determined from the boundary conditions. The boundary condition that requires the magnetic field to be continuous at $x = b$ has been built into the general solutions. Substituting the general solutions into the remaining equations for the boundary conditions yields the following system of equations:

$$\begin{bmatrix} -i\beta & -i\beta & \frac{\omega\epsilon_o\Gamma_p}{n_o q} & \frac{-\omega\epsilon_o\Gamma_p}{n_o q} \\ -i\beta e^{-i\Gamma_h b} & -i\beta e^{i\Gamma_h b} & \frac{\omega\epsilon_o\Gamma_p}{n_o q} e^{-i\Gamma_p b} & \frac{-\omega\epsilon_o\Gamma_p}{n_o q} e^{i\Gamma_p b} \\ i\Gamma_h & -i\Gamma_h & \frac{q\beta}{\omega m} & \frac{q\beta}{\omega m} \\ (i\Gamma_h - \alpha\epsilon_p)e^{-i\Gamma_h b} & -(i\Gamma_h + \alpha\epsilon_p)e^{i\Gamma_h b} & \frac{q\beta}{\omega m} e^{-i\Gamma_p b} & \frac{q\beta}{\omega m} e^{i\Gamma_p b} \end{bmatrix} \begin{bmatrix} H_o \\ H_o R_1 \\ P_o \\ P_o R_2 \end{bmatrix} = \begin{bmatrix} 0 \\ 0 \\ -i\omega\epsilon_o\epsilon_p I_m \frac{\sin\frac{\beta d}{2}}{\frac{\beta d}{2}} \\ 0 \end{bmatrix}$$

The solution for the transformed field components $\mathcal{H}$ and $\mathcal{P}$ can be determined by solving the preceding system of equations for H_o, $H_o R_1$, P_o, and $P_o R_2$, and then substituting the results into the general solutions (33a) to (33d). The result of this operation is

$$\mathcal{H}(x,\beta) = \frac{N(x,\beta)}{D(\beta)} \qquad 0 < x < b \tag{35a}$$

$$\mathcal{P}(x,\beta) = \frac{M(x,\beta)}{D(\beta)} \qquad 0 < x < b \tag{35b}$$

$$\mathcal{H}(x,\beta) = \frac{N(b,\beta)}{D(\beta)} e^{-\alpha(x-b)} \qquad b < x \tag{35c}$$

$$\mathcal{P}(x,\beta) = 0 \qquad b < x \tag{35d}$$

where

$$N(x,\beta) = \frac{i\omega^3 \epsilon_o \epsilon_p \Gamma_p I_m}{\omega_p^2} \frac{\sin \frac{\beta d}{2}}{\frac{\beta d}{2}} \left[\beta^2 \sin \Gamma_h x + \beta^2 \sin \Gamma_h (b - x) \cos \Gamma_p b \right.$$

$$\left. + \frac{\omega^2}{\omega_p^2} \Gamma_h \Gamma_p \cos \Gamma_h (b - x) \sin \Gamma_p b + \alpha \epsilon_p \frac{\omega^2}{\omega_p^2} \Gamma_p \sin \Gamma_h (b - x) \sin \Gamma_p b \right] \quad (35e)$$

$$M(x,\beta) = - \frac{i\omega^2 \epsilon_o \epsilon_p m \beta I_m}{q} \frac{\sin \frac{\beta d}{2}}{\frac{\beta d}{2}} \left[\beta^2 \sin \Gamma_h b \sin \Gamma_p (b - x) - \frac{\omega^2}{\omega_p^2} \Gamma_p \Gamma_h \cos \Gamma_p x \right.$$

$$\left. - \frac{\omega^2}{\omega_p^2} \Gamma_p \Gamma_h \cos \Gamma_h b \cos \Gamma_p (b - x) - \alpha \epsilon_p \frac{\omega^2}{\omega_p^2} \Gamma_p \sin \Gamma_h b \cos \Gamma_p (b - x) \right] \quad (35f)$$

$$D(\beta) = 2\beta^2 \Gamma_h \Gamma_p \frac{\omega^2}{\omega_p^2} \left(1 - \cos \Gamma_h b \cos \Gamma_p b \right) + \left(\beta^4 + \Gamma_p^2 \Gamma_h^2 \frac{\omega^4}{\omega_p^4} \right) \sin \Gamma_h b \sin \Gamma_p b$$

$$- \alpha \epsilon_p \Gamma_p \frac{\omega^2}{\omega_p^2} \left(\beta^2 \sin \Gamma_h b \cos \Gamma_p b + \Gamma_p \Gamma_h \frac{\omega^2}{\omega_p^2} \right) \cos \Gamma_h b \sin \Gamma_p b \quad (35g)$$

The solution for the transformed field is not unique until the proper branches of the double valued parameters Γ_h, Γ_p, and α, as defined by equations (34a) to (34c) are specified. Since both $\mathcal{H}$ and $\mathcal{P}$ are even functions of Γ_h and Γ_p, the choice of either branch for these two parameters will yield the same result for $\mathcal{H}$ and $\mathcal{P}$. The branch of α where $\text{Re}\ \alpha \geq 0$ and $\text{Im}\ \alpha \geq 0$ must be selected to ensure that $\mathcal{H}$ either vanishes at infinity or corresponds to an outward propagating wave. This requirement on α is a consequence of the phase-radiation condition.

The solution for h_y and p can now be determined by employing the inversion integrals (29a) and (29b) where the contour C is shown in figure 2. For $z > 0$, the contour can be closed with a semicircle of infinite radius in the lower half of the β-plane. The contour must be deformed around the branch cut to remain on the proper branch of α. The contour must also be deformed around the poles of the integrands along the real

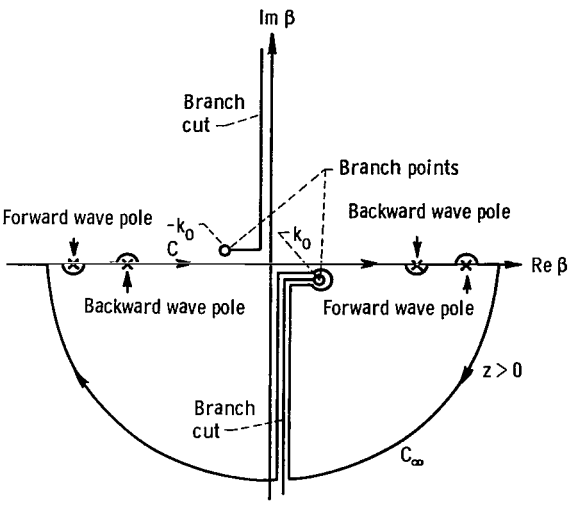

Figure 2. - Complex β-plane.

β-axis. The only poles that should be encircled by the closed contour are the poles that correspond to waves that transport energy away from the source at infinity. This restriction on the contour is imposed by the power-radiation condition. Thus, the forward wave poles located along the positive real β-axis and the backward wave poles located along the negative real β-axis should be encircled. The nature of the poles (i.e., whether they correspond to forward or backward waves) can be determined by computing the phase velocity $v_p = \omega/\beta$ and the group velocity $v_g = \partial\omega/\partial\beta$ of the associated waves. If the product $v_p v_g$ is positive, the wave is a forward wave; whereas, if it is negative, the wave is a backward wave.

It can be shown that the integration over the portion of the contour C_∞ vanishes. Therefore, from Cauchy's theorem, the integral along the contour C is equal to $-2\pi i$ times the sum of the residues of the enclosed poles plus the branch cut integral. Thus,

$$h_y(x,z) = \sum_{n=1}^{N} -\frac{iN(x,\beta_n)}{\left.\frac{\partial D(\beta)}{\partial\beta}\right|_{\beta=\beta_n}} e^{-i\beta_n z} + \text{Branch cut integral} \qquad 0 < x < b \qquad (36a)$$

$$p(x,z) = \sum_{n=1}^{N} -\frac{iM(x,\beta_n)}{\left.\frac{\partial D(\beta)}{\partial\beta}\right|_{\beta=\beta_n}} e^{-i\beta_n z} + \text{Branch cut integral} \qquad 0 < x < b \qquad (36b)$$

$$h_y(x,z) = \sum_{n=1}^{N} -\frac{iN(b,\beta_n)}{\left.\frac{\partial D(\beta)}{\partial\beta}\right|_{\beta=\beta_n}} e^{-\alpha_n(x-b)} e^{-i\beta_n z} + \text{Branch cut integral} \qquad b < x \qquad (36c)$$

$$p(x,z) = 0 \qquad b < x \tag{36d}$$

where the β_n are the roots of $D(\beta) = 0$. The terms in the summations in equations (36a) to (36c) correspond to the discrete spectrum of waves guided by the plasma layer that are often referred to as surface waves, whereas the branch cut integrals correspond to the continuous spectrum of waves of the radiation field. Note that the discrete spectra of h_y and p are identical, as they must be, since the magnetic and pressure fields are coupled by the boundary conditions.

A similar procedure can be carried out to evaluate h_y and p for $z < 0$. For this case, the contour would be closed in the upper half of the β-plane. This completes the formal solution for the field. In order to proceed with the analysis it will be necessary to solve for the roots of $D(\beta) = 0$ and to evaluate the branch cut integrals. These topics will be covered in the following two sections.

DISPERSION CURVES

The roots of the equation $D(\beta) = 0$ can be divided into two groups. In the first group are the roots that correspond to the choice $\text{Re}\ \alpha > 0$. These roots generate physically realizable solutions for the field; that is, they satisfy the radiation condition. The second group contains the roots corresponding to the choice $\text{Re}\ \alpha < 0$. These roots generate solutions that are not physically realizable since they "blow up" at infinity. In this analysis, only the roots in the first group are of interest.

The transcendental equation $D(\beta) = 0$ has both real and complex roots. The loci of these roots in the complex β-plane possess a great deal of symmetry. If $\beta = \beta_{o_2}$ is a root, $\beta = -\beta_o$ is also a root since the variable β always appears in $D(\beta)$ as β^2. This phenomenon should be expected since the plasma medium is isotropic. If a solution is obtained that corresponds to a wave traveling in the positive z-direction, there should also be a similar solution that corresponds to a wave traveling in the negative z-direction. In addition, if $\beta = \beta_o$ is a root of $D(\beta) = 0$, $\beta = \beta_o^*$ is also a root. Because of this symmetry, it is only necessary to determine the roots of $D(\beta) = 0$ in one quadrant of the complex β-plane.

If one is interested in the energy transport along the plasma layer, it is only necessary to compute the real roots of $D(\beta) = 0$. Some of the complex roots may correspond to physically realizable solutions. However, the waves associated with these complex roots cannot transport any net energy. These roots would only be of interest if a calculation of the field pattern in the immediate vicinity of the slot antenna were desired. It should be noted that, if the original equations for a warm plasma contained dissipative effects such as electron-ion collision terms, all the roots of $D(\beta) = 0$ would be complex.

In order to eliminate the tedious numerical work involved in computing the complex zeros of the transcendental function $D(\beta)$, dissipative effects were neglected.

The real roots of $D(\beta) = 0$ were computed on an IBM 7094 computer for various frequencies. It was found that at frequencies below the plasma frequency there are, at most, four real zeros of $D(\beta)$. However, at frequencies above the plasma frequency, the number of real zeros is usually quite large, of the order of $(\omega b/\pi a)\left(1 - \omega_p^2/\omega^2\right)^{1/2}$. To avoid dealing with such a large number of zeros and still cover a reasonable frequency range, unrealistic values must be used for either the plasma layer thickness or electron temperature. Qualitative results for more realistic values of these parameters can then be easily inferred.

The computations were performed for the parameters $\omega_p^2 b^2/c^2 = 5$ and $a/c = 0.1$. The value of $\omega_p^2 b^2/c^2$ corresponds to a plasma layer thickness of $0.35\,\lambda_p$, where λ_p is the free-space wavelength at the plasma frequency, and the value of a/c corresponds to an electron temperature of 37×10^6 °K. The real roots of $D(\beta) = 0$ are shown in figure 3(a) in the form of dispersion curves with λ_o/λ_g as a function of $(\omega/\omega_p)^2$, where

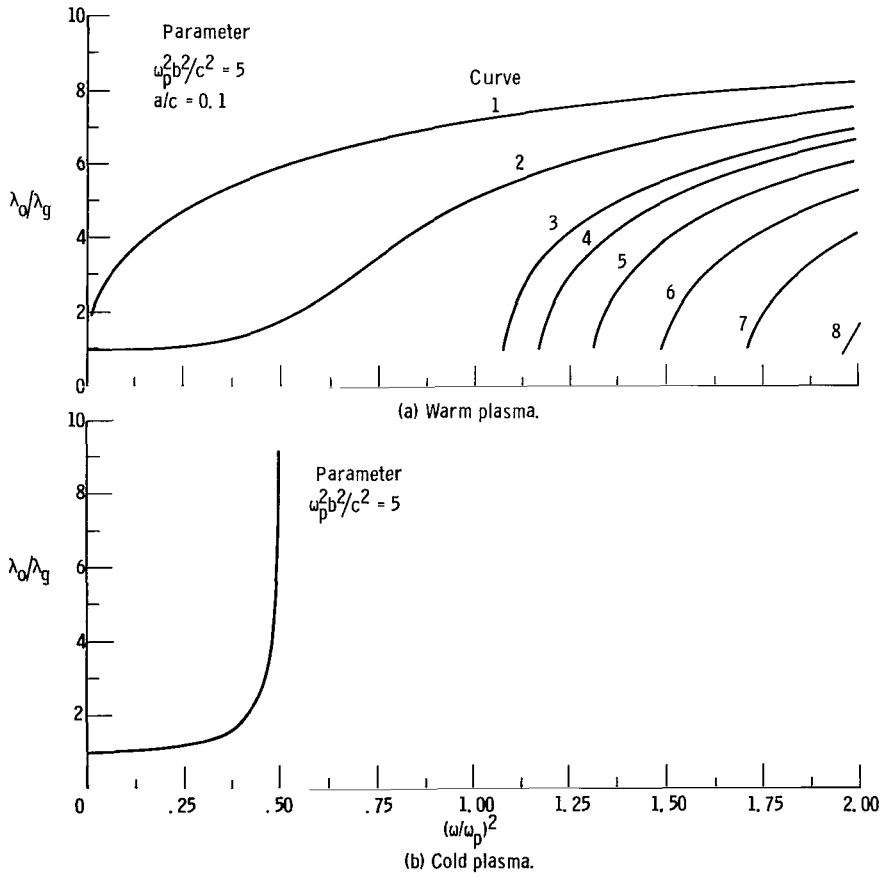

Figure 3. - Dispersion curves for wave coupled to grounded plasma layer.

λ_o is the free-space wavelength of the waves, and λ_g is the wavelength of the guided waves in the plasma layer. (The curves have been numbered for convenience.) Since all the curves are located in the range $1 \leq \lambda_o/\lambda_g \leq c/a$, it can be concluded that the phase velocities associated with the waves are bounded from above by the velocity of light and from below by the electron acoustic velocity. Curves 3 to 8 in figure 3(a) appear to start at points along the line $\lambda_o/\lambda_g = 1$. However, it must be remembered that these curves show only the loci of the real roots of $D(\beta) = 0$ with frequency. At frequencies below the plasma frequency, these roots are complex, which causes the associated waves to be cut off. As the frequency increases, these roots will move in the complex β-plane toward the real β-axis, and at critical frequencies for each root, they will reach the real β-axis at the point $\beta = k_o$. As the frequency further increases, they will rapidly move down the real β-axis away from the origin and asymptotically approach the point $\beta = \omega/a$.

The dispersion curve for the corresponding cold plasma case is shown in figure 3(b), where the cold plasma layer is shown to support only one propagating wave and then only in the frequency range $(\omega/\omega_p)^2 < 0.5$. This result is in sharp contrast with the warm plasma layer that can support several propagating waves at all frequencies. A comparison of figures 3(a) and (b) reveals that curve 2 in the warm plasma case corresponds to the single curve in the cold plasma case in the frequency range $(\omega/\omega_p)^2 < 0.5$. The remaining portion of curve 2 and all the other curves in figure 3(a) are, therefore, unique to the warm plasma layer.

The transverse variations of the magnetic and the pressure fields for the different guided waves (fig. 4) can be determined from the expressions for $N(x, \beta)$ and $M(x, \beta)$, respectively. It can be shown that the wave associated with curve 1 in figure 3(a) is very tightly bound to the plasma-conductor interface; that is, both $N(x, \beta_1)$ and $M(x, \beta_1)$ decrease rapidly in amplitude with increasing x. This wave is essentially the same wave as derived by Seshadri (ref. 9) for the case of a semi-infinite warm plasma bounded by a conducting surface. The wave that corresponds to curve 2 is tightly coupled to the plasma-vacuum interface. All the field components associated with this wave decay rapidly in amplitude as $|x - b|$ deviates from zero. This wave is essentially the same wave as derived by Hessel, et al. (ref. 10) for the case of a semi-infinite warm plasma bounded by a vacuum. The waves associated with curves 3 to 8 are a result of an interaction between the plasma-

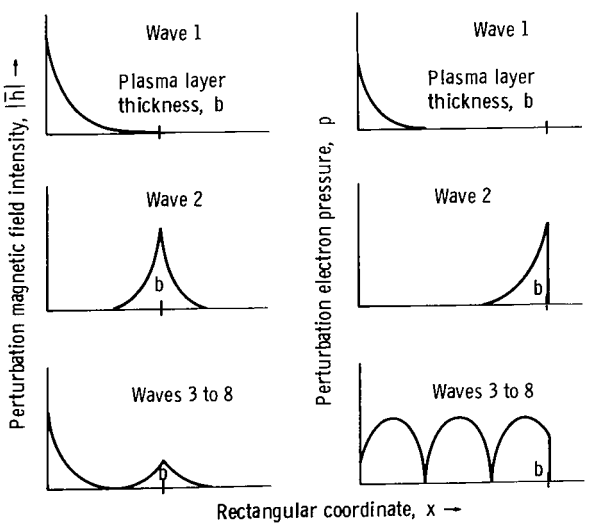

Figure 4. - Typical transverse variations of waves.

conductor and plasma-vacuum interfaces. The magnetic field intensity associated with these waves has its maximum value at either $x = 0$, the plasma-conductor interface, or $x = b$, the plasma-vacuum interface, and it is quite small between these surfaces, whereas the pressure has a standing wave pattern between these two surfaces.

FAR-ZONE RADIATION FIELD

The branch cut integrals give rise to the radiation field. An asymptotic evaluation of the far-zone field will be determined by using the method of saddle-point integration (ref. 11). The solution for the transformed magnetic field in the region $x > b$ is given by equation (35c), which is repeated here for convenience:

$$\mathcal{H}(x, \beta) = \frac{N(b, \beta)}{D(\beta)} e^{-\alpha(x-b)} \tag{35c}$$

The magnetic field h_y is then given by

$$h_y(x, z) = \frac{1}{2\pi} \int_C \frac{N(b, \beta)}{D(\beta)} e^{-\alpha(x-b)} e^{-i\beta z} \, d\beta \qquad x > b \tag{37}$$

where the inversion contour C is shown in figure 2 (p. 21).

At this point, it is convenient to map the complex β-plane into the complex ν-plane with the mapping function

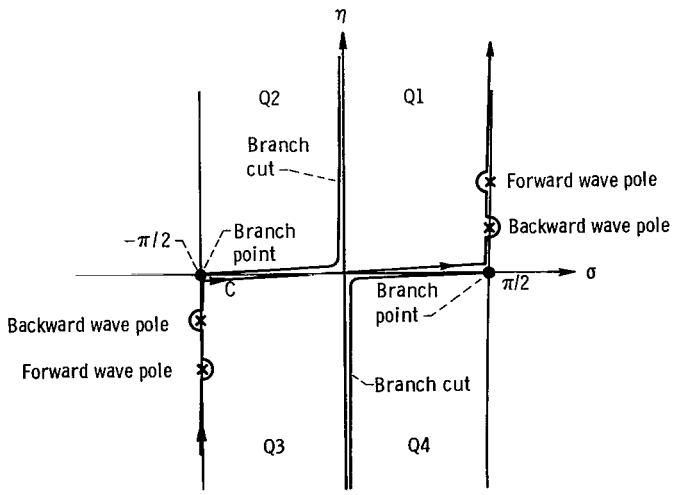

Figure 5. - Complex ν-plane.

$$\beta = k_o \sin \nu \tag{38}$$

where $\nu \equiv \sigma + i\eta$, and to transform x and z into their cylindrical coordinate equivalents with the transformation $z = r \cos \theta$, $x = b + r \sin \theta$ (see fig. 1, p. 10). The mapping of the β-plane into the ν-plane is shown in figure 5. The entire β-plane maps into a strip of width π in the ν-plane. The quantities Q1, Q2, Q3, and Q4 refer to the images of the quadrants of the β-plane in the ν-plane. With these

transformations, the expression for the magnetic field becomes

$$h_y(r,\theta) = \frac{k_o}{2\pi} \int_C \frac{N(b, k_o \sin \nu) \cos \nu \; e^{-ik_o r \sin(\nu+\theta)}}{D(k_o \sin \nu)} \, d\nu \tag{39}$$

The integral for $h_y(r,\theta)$ will be evaluated by the method of saddle-point integration. This method consists of deforming the contour C into a new contour C' so that the magnitude of the exponential term in equation (39) is very small everywhere except in the vicinity of one point along C'. The exponential term will behave much like a delta function in that the value of the integral will be proportional to the value of the integrand at this one point.

The saddle point of the exponent $-ik_o r \sin(\nu + \theta)$ occurs where $\cos(\nu + \theta) = 0$ or where $\nu = \pi/2 - \theta$. In the vicinity of the saddle point $\nu = \pi/2 - \theta$, the function $-ik_o r \sin(\nu + \theta)$ can be expanded in a Taylor series to give

$$-ik_o r \sin(\nu + \theta) = -ik_o r - \frac{k_o r}{2} \rho^2 \sin \varphi \cos \varphi + \ldots$$

where $\rho e^{i\varphi} = \nu - (\pi/2 - \theta)$. The real part of $-ik_o r \sin(\nu + \theta)$ will have the greatest rate of change along the contour that passes through the saddle point at an angle of $\varphi = \pi/4$. This steepest descent contour (SDC) is shown in figure 6.

The exponential term in equation (39) has a unit modulus at $\nu = \pi/2 - \theta$ and falls off as $\exp[-(k_o r/2)\rho^2]$ with distance ρ along the steepest descent contour. If $k_o r \gg 1$, the dominant portion of the integral will be the integrand evaluated at $\nu = \pi/2 - \theta$ times the integral of the Gaussian term with respect to ρ. Thus,

$$h_y(r,\theta) \simeq \frac{k_o}{2\pi} \frac{N(b, k_o \cos \theta) \sin \theta}{D(k_o \cos \theta)} \, e^{-i(k_o r - \pi/4)} \int_{SDC} e^{(-k_o r/2)\rho^2} \, d\rho \tag{40}$$

In evaluating the integral in equation (40), the limits of integration can be selected as $-\infty$ and $+\infty$ since the major contribution to the integral comes from the portion of the contour near $\rho = 0$. Performing the integration gives

$$h_y(r,\theta) \simeq \frac{k_o}{2\pi} \frac{N(b, k_o \cos \theta) \sin \theta \; e^{-i(k_o r - \pi/4)}}{D(k_o \cos \theta)} \left(\frac{2\pi}{k_o r}\right)^{1/2} \tag{41}$$

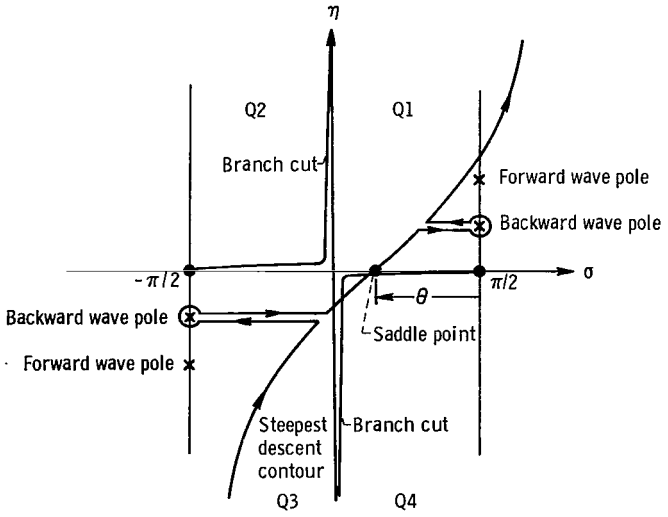

Figure 6. - Steepest descent contour.

If more terms were retained in the expansion of $-ik_o r \sin(\nu + \theta)$, the expression for h_y would contain additional terms of the order $(k_o r)^{-3/2}$ and lower. The additional terms would give a better approximation to the magnetic field h_y especially if $k_o r$ is not extremely large. However, these additional terms do not contribute to any net radiated power.

In deforming the contour C into the steepest descent contour, some of the poles of the integrand may be crossed. This usually happens if the observation angle θ is near 0 or π. It simply indicates that, near the plasma-vacuum interface, the total field also consists of the discrete spectrum of waves.

An interesting phenomenon occurs if one of the poles corresponds to a backward wave. In this case, the steepest descent contour encircles the backward wave pole twice, as shown in figure 6. If $k_o r$ is very large, the effect of these backward wave poles will not be noticed. However, if $k_o r$ is small, the location of the zeros of $D(k_o \sin \nu)$ in equation (39) will have an appreciable effect on the field. The backward wave poles will give rise to a standing wave since two poles are encircled. This standing wave will only be observed for observation angles in the vicinity of $\pi/2$. As the observation angle decreases, a point will be reached where only one of the backward wave poles will be encircled. This is the beginning of the region where the backward waves correspond to traveling waves.

Finally, it should be noted that the steepest descent contour crosses the branch cut in quadrants 2 or 4 of the β-plane. On the improper branch of $\left(\beta^2 - k_o^2\right)^{1/2}$, the contour may encounter the improper or nonspectral roots of $D(k_o \sin \nu) = 0$. The improper roots usually give rise to the dominant portion of the near-zone field (ref. 5). These roots could be used, for example, to evaluate the field along the plasma-vacuum interface. The far-zone field could then be calculated by using a Kirchhoff-Huygens integration over the plasma-vacuum interface. However, the extreme difficulty in obtaining the complex roots of $D(k_o \sin \nu) = 0$ precludes the use of this method.

The shape of the radiation pattern of the far-zone field will be dependent on both the parameters that describe the warm plasma layer and on the width of the slot antenna. Since the modification of the radiation pattern by the warm plasma layer is of interest, it will be expedient to set the width of the slot antenna equal to zero. A slot antenna of zero

width, which is nothing more than a line source, radiates an isotropic field in the absence of a plasma layer. Thus, any deviation from an isotropic pattern when the warm plasma layer is present is entirely a result of the plasma.

The general features of the radiation pattern of the far-zone field can be determined from a study of the functions $N(b, k_o \cos\theta)$ and $D(k_o \cos\theta)$ appearing in equation (41). It can be shown that both $N(b, k_o \cos\theta)$ and $D(k_o \cos\theta)$ are strongly dependent on Γ_h and Γ_p where

$$\Gamma_h = \left(k_e^2 - k_o^2 \cos^2\theta\right)^{1/2} \quad \text{and} \quad \Gamma_p = \left(k_p^2 - k_o^2 \cos^2\theta\right)^{1/2}$$

In particular, the radiation is intense for those directions in space where Γ_h and Γ_p are real, and it is weak for those directions where Γ_h and Γ_p are imaginary.

At frequencies below the plasma frequency k_e^2 and k_p^2 are negative. Since both Γ_h and Γ_p are imaginary for all angles θ in this frequency range, the radiation will be relatively weak. At frequencies above the plasma frequency Γ_h is real for the angles where $k_e^2 - k_o^2 \cos^2\theta > 0$ and Γ_p is real for the angles where $k_p^2 - k_o^2 \cos^2\theta > 0$. Thus, there is a critical angle $\theta_c = \cos^{-1} k_e/k_o = \cos^{-1}\left(\epsilon_p\right)^{1/2}$ c/a associated with Γ_h and a second critical angle $\theta_o = \cos^{-1} k_p/k_o = \cos^{-1}\left(\epsilon_p\right)^{1/2}$ associated with Γ_p. The radiation will generally be weak where $|\cos\theta| > |\cos\theta_c|$, $|\cos\theta| > |\cos\theta_o|$ and strong where $|\cos\theta| < |\cos\theta_c|$, $|\cos\theta| < |\cos\theta_o|$.

At frequencies above the plasma frequency, the critical angle θ_c is always located in physical space since $0 < \left(\epsilon_p\right)^{1/2} < 1$. The critical angle θ_o, however, is usually located in some invisible portion of space since $\left(\epsilon_p\right)^{1/2}$ c/a is usually greater than 1 unless the frequency is very close to the plasma frequency. Since $\left(\epsilon_p\right)^{1/2}$ c/a is usually much greater than 1, variations in the acoustic velocity a will not transform Γ_p from a real to an imaginary quantity. Therefore, variations in the electron temperature should not significantly alter the radiation pattern unless the source frequency is very close to the plasma frequency or the electron temperature is extremely high so that $a/c \sim 1$. These limiting cases have been treated by Stewart and Caron (ref. 6).

Some typical radiation patterns are shown in figure 7 for the frequencies $\left(\omega/\omega_p\right)^2 = 0.1$ and 2.0. The radiation patterns have been normalized by setting the intensity in the direction $\theta = \pi/2$ equal to 1. Because of the symmetry of the structure, only the range of angles $0 < \theta < \pi/2$ has to be considered.

The radiation pattern is not affected by variations in the electron temperature as long as the temperature is sufficiently low so that $a/c \leq 10^{-3}$ except for the special case where the source frequency is extremely close to the plasma frequency. For higher temperatures, the pattern is slightly changed, as shown in figure 7. The shapes of the

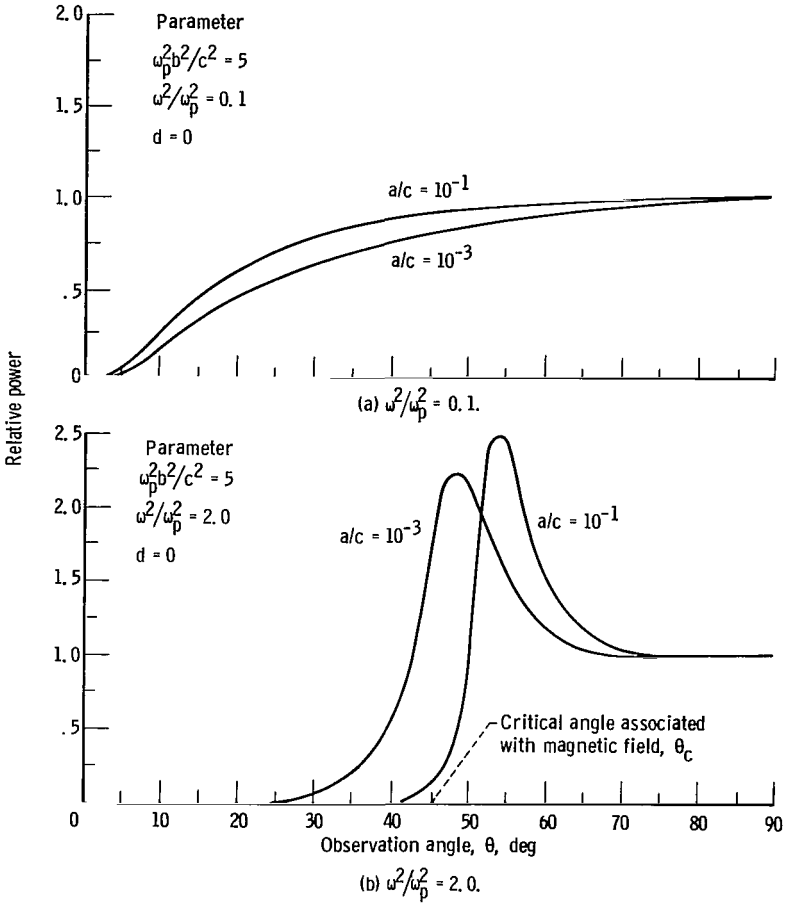

Figure 7. - Radiation pattern of far-zone field.

radiation patterns can be easily explained from ray theory by using the cold plasma model (e.g., see ref. 3).

If the width of the slot antenna were nonzero, the intensity of the radiation field in the direction θ would be reduced by the factor

$$\left| \frac{\sin\left(\frac{k_o d}{2} \cos\theta\right)}{\frac{k_o d}{2} \cos\theta} \right|^2$$

The reduction in field intensity in all directions is not large unless $k_o d$ exceeds 1. A typical value for $k_o d/2$ is of the order 0.2, which corresponds to a slot width of 0.1 λ_o, where λ_o is the free-space wavelength at the source frequency. Thus, it can be

concluded that the radiation patterns, as shown in figure 7, are typical of patterns that are associated with a plasma-covered slot antenna.

ENERGY TRANSPORTED BY THE FIELD

The final topic to be considered is the energy transported by the field. In an ordinary dielectric medium, the energy transport can be computed by using the Poynting vector. To determine how the Poynting vector should be modified to include the effects present in a warm plasma, consider the divergence of $\bar{e} \times \bar{h}^* + p\bar{v}^*$:

$$\nabla \cdot \left(\bar{e} \times \bar{h}^* + p\bar{v}^*\right) = \left(\nabla \times \bar{e}\right) \cdot \bar{h}^* - \left(\nabla \times \bar{h}^*\right) \cdot \bar{e} + p\nabla \cdot \bar{v}^* + \left(\bar{v}^* \cdot \nabla\right) p \tag{42}$$

The right side of equation (42) can be simplified by using the basic equations (11) to (14). The result of this simplification is

$$\nabla \cdot \left(\bar{e} \times \bar{h}^* + p\bar{v}^*\right) = -4i\omega \left(\frac{\mu_o \bar{h} \cdot \bar{h}^*}{4} - \frac{\epsilon_o \bar{e} \cdot \bar{e}^*}{4} - \frac{pp^*}{4mn_o a^2} + \frac{n_o m \bar{v} \cdot \bar{v}^*}{4} \right) - 2\left(\frac{\bar{h}^* \cdot \bar{j}_m}{2} \right) \tag{43}$$

The terms in the first parentheses on the right in equation (43) are energy storage terms. They are the magnetic, electric, electron potential, and electron kinetic energy densities, respectively. The last term in equation (43) represents the energy loss due to the magnetic currents. Equation (43) can be put into the following form by using the divergence theorem:

$$\frac{1}{2} \operatorname{Re} \oint_S \left(\bar{e} \times \bar{h}^* + p\bar{v}^*\right) \cdot d\bar{S} = - \int_V \frac{1}{2} \bar{h}^* \cdot \bar{j}_m \, dV \tag{44}$$

Since the right side of equation (44) represents the rate at which energy is being dissipated in the volume V, the left side of equation (44) must be the rate at which energy is being supplied to V. Thus, it is proper to interpret the quantity $\bar{S} = \frac{1}{2} \operatorname{Re}(\bar{e} \times \bar{h}^* + p\bar{v}^*)$ as the energy flux vector for a warm plasma medium. The energy flux vector $\bar{S}$ is simply the sum of the usual Poynting vector $\bar{e} \times \bar{h}^*$, which accounts for the electromagnetic energy transport, and the term $p\bar{v}^*$, which accounts for the energy transport due to the electron motion.

Next, consider the power orthogonality properties of the guided waves. Assume that

there are two guided waves having the components $\{\bar{e}_1, \bar{h}_1, p_1, \bar{v}_1, \beta_1\}$ and $\{\bar{e}_2, \bar{h}_2, p_2, \bar{v}_2, \beta_2\}$ that propagate along the plasma layer. The total power associated with these waves per unit length in the y-direction is given by

$$P_{total} = P_1 + P_2 + P_{12} \tag{45a}$$

where

$$P_i = \frac{1}{2} \mathrm{Re} \int_0^\infty \left(\bar{e}_i \times \bar{h}_i^* + p_i \bar{v}_i^* \right) \cdot \hat{a}_z \, dx \tag{45b}$$

and

$$P_{ij} = \frac{1}{2} \mathrm{Re} \int_0^\infty \left(\bar{e}_i \times \bar{h}_j^* + \bar{e}_j \times \bar{h}_i^* + p_i \bar{v}_j^* + p_j \bar{v}_i^* \right) \cdot \hat{a}_z \, dx \tag{45c}$$

It is obvious that P_i is the total power associated with the i^{th} wave if it alone were present. It is expected that $P_{ij} = 0$ if $\beta_i \neq \beta_j$. The fact that P_{ij} is zero if $\beta_1 \neq \beta_j$ can be shown in several ways. First, general expressions for $\bar{e}$ and $\bar{v}$ in terms of $\bar{h}$ and p could be substituted into equation (45c). The integration could then be carried out by parts giving quantities that are evaluated only at the end points. Employing the boundary conditions will require these end-point quantities to vanish.

A second approach to the problem is to recognize that, for the case where there are no energy losses due to dissipative effects such as collisions, the total power associated with the waves must be independent of the z-coordinate. Since both P_1 and P_2 are independent of z, it must follow that P_{12} is also independent of z. In forming P_{12}, terms like $e^{-i(\beta_1 - \beta_2)z}$ and $e^{i(\beta_1 - \beta_2)z}$ appear in the integrand (for the assumption that β_1 and β_2 are real). Therefore, if P_{12} is to be independent of z, either the coefficients of the preceding terms must vanish or $\beta_1 = \beta_2$. However, since $\beta_1 \neq \beta_2$ the coefficients of these terms vanish making $P_{12} = 0$.

This proof can easily be extended to show that the power associated with the continuous portion of the spectrum is also orthogonal to the powers of all the discrete waves. The continuous spectrum can simply be regarded as the superposition of an infinite number of discrete waves. The powers of each of these waves must be orthogonal to every member of the discrete spectrum since the range of β for the continuous spectrum does not include members of the discrete spectrum. Therefore, the total energy transported by the field is simply the sum of the energies transported by each member of the discrete spectrum plus the energy transported by the waves of the continuous spectrum.

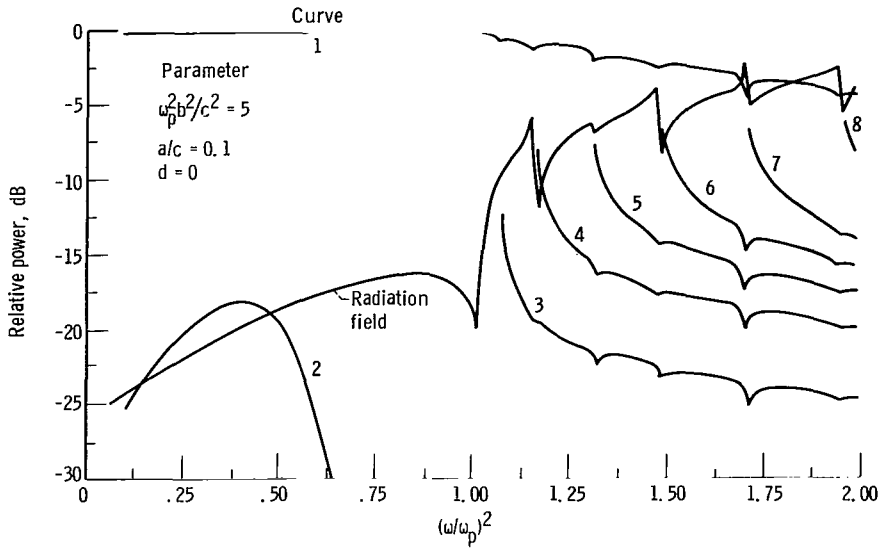

Figure 8. - Relative powers associated with waves.

The energy flux density vector $\bar{S}$ was evaluated for each of the guided waves and the radiation field. The energy transported by a guided wave was computed by integrating the corresponding vector $\bar{S}$ over a surface normal to the z-axis and extending over the range $0 \leq x \leq \infty$ and $0 \leq y \leq 1$. This result was then doubled, since for every guided wave propagating in the positive z-direction there will be an identical wave propagating in the negative z-direction. The energy transported by the radiation field was computed by integrating the corresponding vector $\bar{S}$ over a segment of a cylindrical surface of infinite radius extending over the range $0 \leq \theta \leq \pi/2$ and $0 \leq y \leq 1$. This result was then doubled, since the pattern of the radiation field is symmetrical about $\theta = \pi/2$.

Numerical results for the energy transport are presented in figure 8 for the parameters $\omega_p^2 b^2/c^2 = 5$, $a/c = 0.1$, and $d = 0$. It is instructive to consider first the case where the slot antenna has zero width (i.e., $d = 0$) and later extend the results to include the effect of a varying slot width. The power associated with each wave is expressed as a ratio in decibels of the wave power to the total power supplied by the source. The curves in figure 8 are numbered for easy comparison with the dispersion curves in figure 3(a)(p. 23).

The results show that, at frequencies below the plasma frequency, the dominant mechanism for transporting energy is wave 1, the wave coupled to the plasma-conductor interface. The radiation field and wave 2, the wave coupled to the plasma-vacuum interface, each account for about 1 percent of the total power.

The nature of these results should be expected. The wave coupled to the plasma-vacuum interface decays very rapidly with distance from the interface. Consequently, there will be very little coupling between this wave and the source. The wave coupled to the plasma-conductor interface, however, is very intense at the location of the source

and, therefore, is strongly excited. The radiation field is weakly excited since the plasma layer is quite thick and opaque to electromagnetic waves in this frequency range.

At frequencies above the plasma frequency, the radiation field is more strongly excited. However, wave 1 still accounts for the major portion of the power until $\left(\omega/\omega_p\right)^2$ exceeds about 1.7. At the onset of propagation of waves 3 to 8, the relative intensity of the radiation field takes a sharp drop. As the frequency increases, the fraction of the total energy that is transported by these additional waves drops quite rapidly allowing the relative intensity of the radiation field to increase. Even though the number of these additional waves increases quite rapidly with frequency, the relative amount of energy that they transport is decreasing. Thus, in the limit of infinite frequency all the energy will be transported by the radiation field regardless of the electron temperature.

In the cold plasma model, the radiation field transports all the energy at frequencies where $\left(\omega/\omega_p\right)^2 > 0.5$, since no propagating guided waves can exist in this frequency range. This is in sharp contrast to the results for the warm plasma model. The radiation field in the warm plasma model accounts for only 1 percent of the total power supplied by the source at $\left(\omega/\omega_p\right)^2 = 0.5$ and about 50 percent of the total power at $\left(\omega/\omega_p\right)^2 = 2$.

It must be remembered that the numerical results are for an extremely high electron temperature. However, the results demonstrate that the electron temperature can have an appreciable effect on the intensity of the radiation field. A limited amount of numerical work has been done by using more realistic values for the electron temperature. For the case where $\omega_p^2 b^2/c^2 = 4.0\times10^{-3}$ and $a/c = 2\times10^{-3}$, which corresponds to a plasma layer thickness of $0.01\ \lambda_p$ and an electron temperature $15\times10^3\ ^oK$, it was found that wave 1, the wave coupled to the plasma-conductor interface, still accounts for the major portion of the power supplied by the source in the frequency range $\left(\omega/\omega_p\right)^2 < 1$ even though the plasma layer is extremely thin. Thus, it can be concluded that at frequencies below the plasma frequency the wave coupled to the plasma-conductor interface is the dominant energy-transport mechanism for the case where the slot antenna has zero width.

If the slot antenna has a finite width the power of the n^{th} guided wave will be reduced by the factor

$$\left| \frac{\sin \frac{\beta_n d}{2}}{\frac{\beta_n d}{2}} \right|^2$$

If the guided wave amplitudes are to be significantly reduced, the slot width d must be sufficiently large so that $\beta_n d/2 = \pi d/\lambda_g > \pi$. Since λ_o/λ_g is of the order c/a for each

of the guided waves except in the vicinity of their low frequency cutoff points (see fig. 3, p. 23), the condition for a significant reduction in guided wave amplitudes can be stated as $d/\lambda_o > a/c$. Since a/c is usually in the range 10^{-3} to 10^{-5}, the condition $d/\lambda_o > a/c$ is readily satisfied. It has been shown in a previous section that the finite width of the source will not distort or attenuate the far-zone field if $k_o d < 1$. Therefore, it can be concluded that for the case of a slot antenna of finite width the dominant energy-transport mechanism is the radiation field except at frequencies near the guided wave cutoff frequencies.

CONCLUSIONS

The radiation from a slot antenna in a ground plane covered by a warm plasma layer has been determined. The radiation pattern of the far-zone field was not affected by the plasma temperature unless the source frequency was near the plasma frequency or the plasma temperature was extremely high so that the electrons have relativistic thermal velocities. The complete spectrum of waves guided by the warm plasma layer was also determined. The spectrum of waves associated with a warm plasma layer was significantly different from the spectrum associated with a cold plasma layer. The energy transported by the guided waves often greatly exceeded the energy transported by the radiation field for the case where the slot antenna had zero width. However, the radiation field proved to be the dominant energy-transport mechanism for the case where the slot antenna had a finite width.

Lewis Research Center,
National Aeronautics and Space Administration,
Cleveland, Ohio, March 28, 1966.

REFERENCES

1. Kuhns, Perry W.: Effect of Addition of Impurities on Electron-Ion Recombination Times and on Transmission Through Ionized Layers. Electromagnetic Aspects of Hypersonic Flight, W. Rotman, H. K. Moore, and R. Papa, eds., Spartan Books, Inc., 1964, pp. 12-21.

2. Rothman, H.; Morita, T.; and Scharfman, W.: Transmission Through an Ionized Medium in the Presence of a Strong Magnetic Field. Electromagnetic Aspects of Hypersonic Flight, W. Rotman, H. K. Moore, and R. Papa, eds., Spartan Books, Inc., 1964, pp. 196-212.

3. Omura, Masayuki: Radiation Pattern of a Slit in a Ground Plane Covered by a Plasma Layer. Rept. No. AFCRL-62-958, Air Force Cambridge Res. Labs., Dec. 1962.

4. Tamir, T.; and Oliner, A. A.: The Spectrum of Electromagnetic Waves Guided by a Plasma Layer. IEEE Proc., vol. 51, no. 2, Feb. 1963, pp. 317-332.

5. Tamir, T.; and Oliner, A. A.: The Influence of Complex Waves on The Radiation Field of a Slot-Excited Plasma Layer. IRE Trans. on Antennas and Propagation, vol. AP-10, no. 1, Jan. 1962, pp. 55-65.

6. Stewart, G.; and Caron, P.: Radiation from a Line Source in a Ground Plane Covered by a Warm Plasma Slab. IEEE Trans. on Antennas and Propagation, vol. AP-13, no. 4, July 1965, pp. 600-611.

7. Oster, L.: Linearized Theory of Plasma Oscillations. Rev. Modern Phys., vol. 32, no. 1, Jan. 1960, pp. 141-168.

8. Oliner, A. A.; and Tamir, T.: Radiation from Semi-Infinite Slot-Excited Plasma-Sheath Configurations. Electromagnetic Aspects of Hypersonic Flight, W. Rotman, H. K. Moore, and R. Papa, eds., Spartan Books, Inc., 1964, pp. 32-49.

9. Seshadri, S. R.: Radiation from an Electromagnetic Source in a Half-Space of Compressible Plasma-Surface Waves. IEEE Trans. on Antennas and Propagation, vol. AP-12, no. 3, May 1964, pp. 340-348.

10. Hessel, A.; Markuvitz, N.; and Shmoys, J.: Scattering and Guided Waves at an Interface Between Air and a Compressible Plasma. IRE Trans. on Antennas and Propagation, vol. AP-10, no. 1, Jan. 1962, pp. 48-54.

11. Collin, Robert E.: Field Theory of Guided Waves. McGraw-Hill Book Co., Inc., 1960, pp. 495-506.

"The aeronautical and space activities of the United States shall be conducted so as to contribute . . . to the expansion of human knowledge of phenomena in the atmosphere and space. The Administration shall provide for the widest practicable and appropriate dissemination of information concerning its activities and the results thereof."

—NATIONAL AERONAUTICS AND SPACE ACT OF 1958

NASA SCIENTIFIC AND TECHNICAL PUBLICATIONS

TECHNICAL REPORTS: Scientific and technical information considered important, complete, and a lasting contribution to existing knowledge.

TECHNICAL NOTES: Information less broad in scope but nevertheless of importance as a contribution to existing knowledge.

TECHNICAL MEMORANDUMS: Information receiving limited distribution because of preliminary data, security classification, or other reasons.

CONTRACTOR REPORTS: Technical information generated in connection with a NASA contract or grant and released under NASA auspices.

TECHNICAL TRANSLATIONS: Information published in a foreign language considered to merit NASA distribution in English.

TECHNICAL REPRINTS: Information derived from NASA activities and initially published in the form of journal articles.

SPECIAL PUBLICATIONS: Information derived from or of value to NASA activities but not necessarily reporting the results of individual NASA-programmed scientific efforts. Publications include conference proceedings, monographs, data compilations, handbooks, sourcebooks, and special bibliographies.

Details on the availability of these publications may be obtained from:

SCIENTIFIC AND TECHNICAL INFORMATION DIVISION

NATIONAL AERONAUTICS AND SPACE ADMINISTRATION

Washington, D.C. 20546